Deep levels in p^+-n junctions fabricated by rapid thermal annealing of Mg or Mg/P implanted InP

L. Quintanilla,[a] S. Dueñas, E. Castán, R. Pinacho, and J. Barbolla
Departamento de Electricidad y Electrónica, Facultad de Ciencias, Universidad de Valladolid, 47011 Valladolid, Spain

J. M. Martín and G. González-Díaz
Departamento de Electricidad y Electrónica, Facultad de Físicas, Universidad Complutense, 28040 Madrid, Spain

(Received 15 October 1996; accepted for publication 2 January 1997)

In this work, we investigate the deep levels present in ion implanted and rapid thermal annealed (RTA) InP p^+-n junctions. The samples were implanted with magnesium or coimplanted with magnesium and phosphorus. These levels were characterized using deep level transient spectroscopy (DLTS) and capacitance–voltage transient technique (CVTT). Seven majority deep levels located in the upper half of the band gap were detected in the junctions by using DLTS measurements, four of which (at 0.6, 0.45, 0.425, and 0.2 eV below the conduction band) result from RTA, while the origin of the other three levels (at 0.46, 0.25, and 0.27 eV below the conduction band) can be ascribed to implantation damage. An RTA-induced origin was assigned to a minority deep level at 1.33 eV above the valence band. From CVTT measurements, several characteristics of each trap were derived. Tentative assignments have been proposed for the physical nature of all deep levels. © *1997 American Institute of Physics.* [S0021-8979(97)03407-5]

I. INTRODUCTION

Indium phosphide has become a compound semiconductor of considerable interest from a technological viewpoint. It has been an excellent candidate for the fabrication of optoelectronic, microwave, and high-power and high-speed electronic devices, due to its outstanding physical properties, such as the high electron mobility and high breakdown field.

Ion implantation combined with subsequent rapid thermal annealing (RTA) seems to be a promising doping technology for InP. In particular, p-type implants are required in device applications to obtain low specific contact resistance or sharp p^+-shallow gates in junction field effect transistors.[1,2] For this kind of implant, electrical activation is usually less than 50%, and the maximum achievable hole concentration is about 5×10^{18} cm^{-3}.[3] In addition, a broadening of the implant profile as well as an inward and outward diffusion of p-type dopants (Be, Mg, and Zn) are detected after elevated temperature treatments even when RTA is employed.[4] In order to achieve sharp p-type profiles, some authors have proposed the use of coimplantation of electrically inactives species, such as Ar, or complementary species, such as P, as an alternative to single-species implantation.[5–8]

The main disadvantage of ion implantation is the introduction of lattice damage in the semiconductor resulting in high densities of deep levels. On the other hand, RTA-induced defects in InP have been illustrated in the literature,[9,10] which are believed to be either intrinsic defects or impurity-related defects activated by the thermal annealing. Because of the large number of residual impurities existing in unintentionally doped InP[11] and their migration during thermal treatments,[11,12] special attention should be paid to these last defects.

One of the main questions about ion implantation, from the viewpoints of the fabrication process and optimization of semiconductor devices, is the characterization of the residual damage after annealing in regions located not only near the p-n junction or at the implanted layer, but also deeper into the bulk. In addition to conventional DLTS, the capacitance–voltage transient technique (CVTT) has been shown[13–15] to be a useful method to characterize the deep levels existing in semiconductor materials even when DLTS is complicated by systematic distortions.

The main aim of this work is to study the deep levels located in the upper half of the band gap in InP p^+-n junctions produced by Mg implantation and subsequent rapid thermal annealing. In order to establish the effect of coimplantation on the junction characteristics and on the trap distributions, Mg/P dual implantations were carried out. A special effort was also devoted to determining the trap origin: whether the starting material or the sequential steps in the diode fabrication technological processes. A detailed discussion about their physical origin has been carried out in order to propose tentative assignations.

II. SAMPLE DESCRIPTION

The substrates used in this work were undoped n-type LEC-grown InP from MCP Ltd. with a net unintentional dopant concentration of 1×10^{15} cm^{-3} measured by using standard $C-V$ profiling at room temperature.

The upper 300-nm-thick p^+ layers were produced by Mg implantation at 80 keV with a dose of 1×10^{14} cm^{-2}. In order to study P coimplantation effects, ion implantation of this element was carried out at 120 keV with a dose of 1×10^{14} cm^{-2}, which results in overlapping profiles with those of the

[a]Electronic mail: luisq@alpha2.ele.cie.uva.es

Copyright ©2001. All Rights Reserved.

Mg implantation. All implantations were performed at room temperature with the substrates tilted 7° with respect to the beam to avoid channeling effects.

The samples were RTA annealed by using a commercial system from MPT Corp. equipped with graphite susceptor. During annealing, samples were placed face down on a Si wafer. The annealing was done at 875 °C for 5 s in flowing Ar, which resulted in layers with excellent crystalline quality and surface morphology.[8]

Ohmic contacts for the n- and p^+-type layers were produced using evaporated AuGe/Au and AuZn/Au, respectively, alloyed at 420 °C for 1 min.

The junctions were defined by conventional photolitography methods with different areas. The results presented in this article correspond to devices having an area of 500×500 μm^2. Isolation between devices was obtained by wet etching using a solution of 1 H_2O_2:1 H_2SO_4.

In order to be able to separate the effects of ion implantation from those of RTA processing or even the potential native defects of the ''as-grown'' compound semiconductor, control samples were always kept for comparison: one unimplanted, non-RTA treated n-type InP sample and one unimplanted sample subjected to an RTA process of 875 °C for 5 s were used. Schottky diodes on these crystals were produced by evaporation of a 300-nm-thick gold film in an ultrahigh vacuum system.

III. EXPERIMENTAL TECHNIQUES

DLTS measurements were performed using a Boonton 72B capacitance meter and a Tektronix TDS 320 digital oscilloscope was used to record the complete capacitance transients. The filling pulses were introduced using a Tektronix PG2010 pulse generator. A reverse bias of 2 V was pulsed back to 0 and to 0.5 V forward bias for 10 ms to investigate majority (electron) and minority (hole) traps, respectively, involving a region in the n side of the junction that extends between 1 and 2 μm from the junction. Samples were cooled in darkness from room temperature to 78 K at zero bias in an Oxford DN1710 cryostat.

DLTS is a widely used technique that has proven to be very useful because of its high sensitivity and ease of interpretation. Yet, it has been evidenced that it is complicated when transients become nonexponential as a consequence of different effects that take place in the space-charge region of the junction, for example: the Poole–Frenkel effect, nonhomogeneous distributions of shallow impurities and/or deep levels, refilling effects in the edge zone of the space-charge region, and so on.[16,17] On the other hand, the DLTS technique provides information about the defects in the portion of the depletion region scanned with the corresponding pulse height. Thus, ''average'' information about the simultaneous processes that are occurring throughout this region is obtained. In order to determine the spatial distribution of some trap characteristics, such as their emission coefficient or concentration, point-to-point across the space-charge region, the capacitance–voltage transient technique (CVTT) was used. This technique has been described elsewhere.[13]

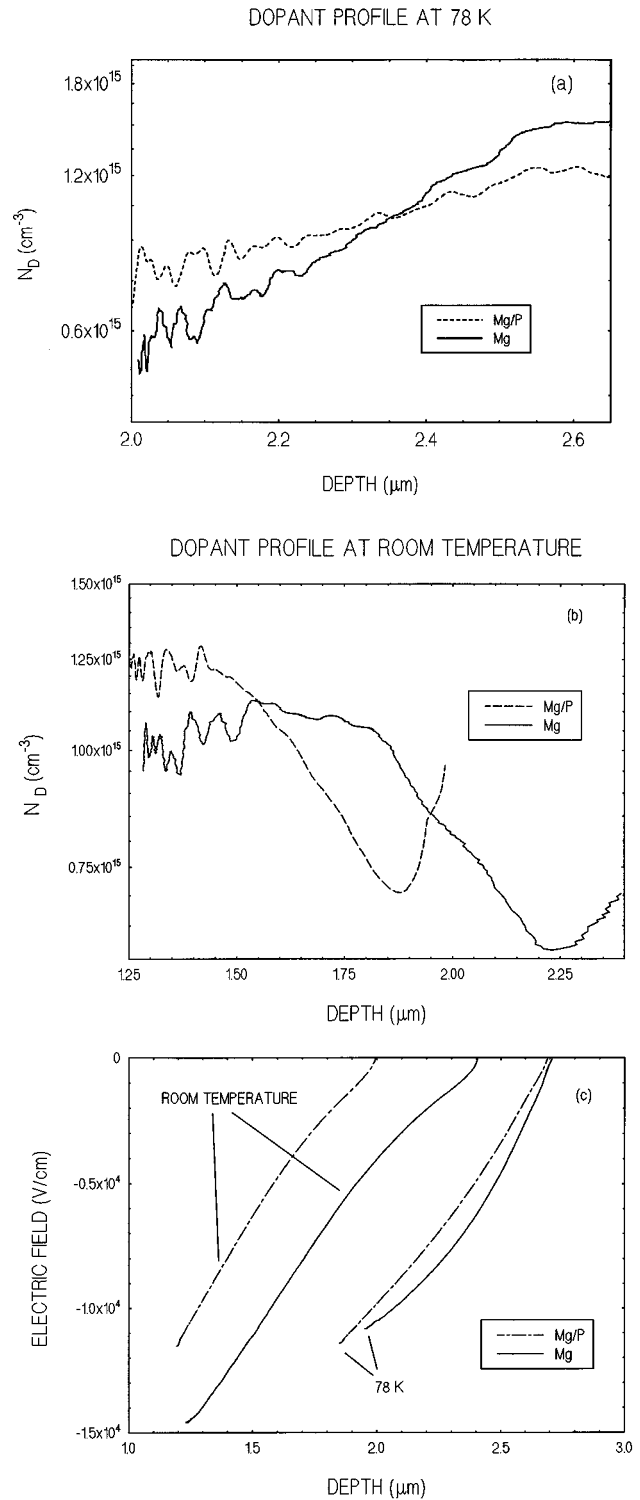

FIG. 1. (a) and (b) Dopant profiles for Mg and Mg/P implanted samples at 78 K and at room temperature. (c) Electric field distributions across the space-charge region corresponding to the (a) and (b) dopant profiles. For all the curves, the emission time was selected to be high enough so that emission transients were saturated.

IV. EXPERIMENTAL RESULTS AND DISCUSSION

Figures 1(a) and 1(b) show the dopant profiles of the implanted samples obtained by using CVTT at 78 K, at which all deep levels are filled with electrons, and at room

Copyright ©2001. All Rights Reserved.

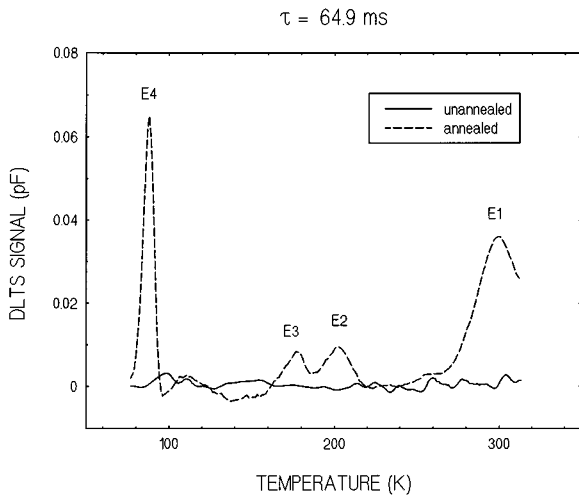

FIG. 2. Majority DLTS spectra for the control samples.

temperature, at which all levels are emptied. Thus, the relation between the total trap concentration and the dopant concentration can be estimated. As can be seen from these curves, only a small contribution of the deep levels to the total dopant concentration is suggested. One important observation is that at 78 K the dopant profiles have a nonuniform distribution, increasing toward the bulk, and with a higher gradient for the Mg implanted sample. Thus we can conclude that the coimplantation process provides a more abrupt junction. This result agrees with SIMS profiles reported previously.[18]

In Fig. 1(c), the electric field distributions obtained by integrating these profiles have been plotted. The nonuniform distribution of dopants detected at low temperature produces a nonlinear dependence of the electric field distribution across the space-charge region, as it corresponds to a gradually doped junction. This behavior is more apparent in the Mg-implanted sample where the junction occurs more gradually. At room temperature, the electric field distributions show an almost linear dependence, corresponding to a uniform dopant distribution. The slope change observed at the lowest values of the field is due to the fact that in this zone (Debye tail region), a nonzero free electron concentration exists that compensates the dopant charge density. Regarding the electric field values, at 78 K, the absolute values are similar in both samples, which could indicate a similar concentration of ionized centers below this temperature. On the contrary, at room temperature a clear difference is noticed, which may be caused by a higher concentration of ionized levels at this temperature for the Mg-implanted samples.

In Fig. 2, DLTS spectra of the unimplanted and unannealed sample and the RTA-annealed sample are shown. As can be seen, no deep levels were found in the unannealed sample by using DLTS. This result was confirmed by the overlapping of the dopant profiles obtained by standard C–V profiling recorded at room temperature and at 78 K. In contrast, thermal treatment brings about four electron traps whose corresponding energies are the following: $E_{E1}=E_C-0.6$ eV, $E_{E2}=E_C-0.45$ eV, $E_{E3}=E_C-0.425$ eV, $E_{E4}=E_C-0.21$ eV. Indeed, because these samples are

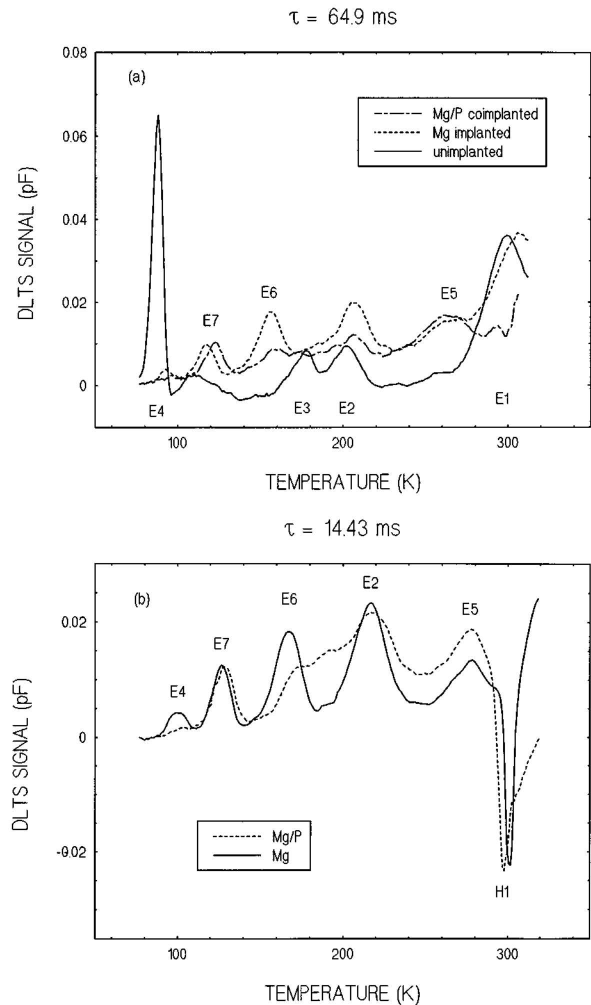

FIG. 3. (a) Majority DLTS spectra for the Mg and Mg/P implanted p^+-n junctions. DLTS spectrum for the annealed, unimplanted sample was also included for comparison. (b) Minority DLTS spectra for the Mg and Mg/P implanted p^+-n junctions. A 400 μA/mm^2 forward current pulse was injected during 10 ms.

Schottky barriers, only majority carrier defects are revealed.

DLTS spectra for electron traps of Mg-implanted and Mg/P coimplanted samples have been presented in Fig. 3(a), along with that of the annealed and unimplanted sample for comparison. Up to six electron traps were detected with the following emission energies: $E_{E1}=E_C-0.6$ eV, $E_{E2}=E_C-0.45$ eV, $E_{E4}=E_C-0.2$ eV, $E_{E5}=E_C-0.46$ eV, $E_{E6}=E_C-0.25$ eV, and $E_{E7}=E_C-0.27$ eV. Due to their similar energy and peak position, the levels E1, E2, and E4 seem to be the same as the levels induced by the RTA process. It is important to note that the E4 peak amplitude decreases with respect to that of unimplanted samples. As a consequence, a lower E4 deep-level concentration in the implanted samples is indicated. Furthermore, three new traps (E5, E6, and E7) were detected, whereas E3 vanished.

Minority DLTS spectra of the implanted samples were measured and the results are shown in Fig. 3(b). All the above deep levels were observed with the exception of E1. This center was replaced by a negative peak that corresponds to a hole trap (H1) whose corresponding energy and concentration were estimated by $E_{H1}=E_v+1.33$ eV and

Copyright ©2001. All Rights Reserved.

$N_{TH1} \approx 0.8-1.5\times10^{14}$ cm^{-3}, respectively. This level might be the same level involved in the 1.3 eV transition reported by photoluminiscence measurements in a previous work.[8]

Using the DLTS results, the deep levels can be ascribed in two groups related to the technological process responsible for their origin: RTA induced centers (E1, E2, E3, and E4) and ion-implantation induced centers: E5, E6, and E7 levels. As minority DLTS spectra cannot be recorded in annealed and unimplanted samples, no comparison between the RTA only process and the RTA plus implantation process can be made. So, at this stage of the study, we cannot propose any origin for the H1 trap.

CVTT curves recorded at temperatures near DLTS maxima provide information about each particular center. From their analysis, several characteristics of each trap were derived in order to obtain further insight into its physical nature. In order to compare the experimental results, CVTT curves for each center in different samples were recorded at the same temperature. The discussion is organized according to the considered deep-level properties: damage concentration profile and emission coefficients.

A. Damage concentration profile

1. E1 and H1 levels

Regarding the origin of the E1 trap at 0.6 eV, Fe is an impurity present in undoped InP that introduces an acceptor level at an energy of 0.6–0.65 eV,[19] which matches the energy of E1. The outward-diffusion mechanism of Fe induced by high temperature processes[11] can explain the existence of the center, only after the RTA treatment.

The E1 emission transients of the implanted samples obtained by CVTT display an anomalous behavior, as shown in Fig. 4(a) for the Mg-implanted sample at two different points of the depletion region. After an apparently normal initial part of the transient, they become ''collapsed'' in certain points of the space-charge region and, eventually, they recover their amplitudes. This behavior was also found in the annealed and unimplanted sample.

At this point, we must keep in mind the existence of the E1 and H1 deep levels, both appearing at nearly the same temperature range. We propose the following mechanism to explain this distortion: at the beginning of the transient, electrons trapped at the E1 center are emitted and reach the conduction band. As the H1 center is located very near this band, the capture of these electrons by the H1 deep level may be energetically favored, yielding a decreasing transient.

From these transients, reliable damage profiles and emission rate distributions across the depletion region cannot be derived. The damage profile obtained from the transient amplitude [Fig. 4(b)] can only be considered as ''apparent.'' As can be seen, the profiles show a similar behavior with a relatively uniform concentration and a clear depletion at well-located space-charge region points. Finally, they tend to recover their original values. At the depletion points, the electron capture due to H1 becomes dominant. Following this idea, the depletions found in the dopant profiles at room temperature [Fig. 1(b)] may be interpreted as a result of the H1 ionization change during its capture process.

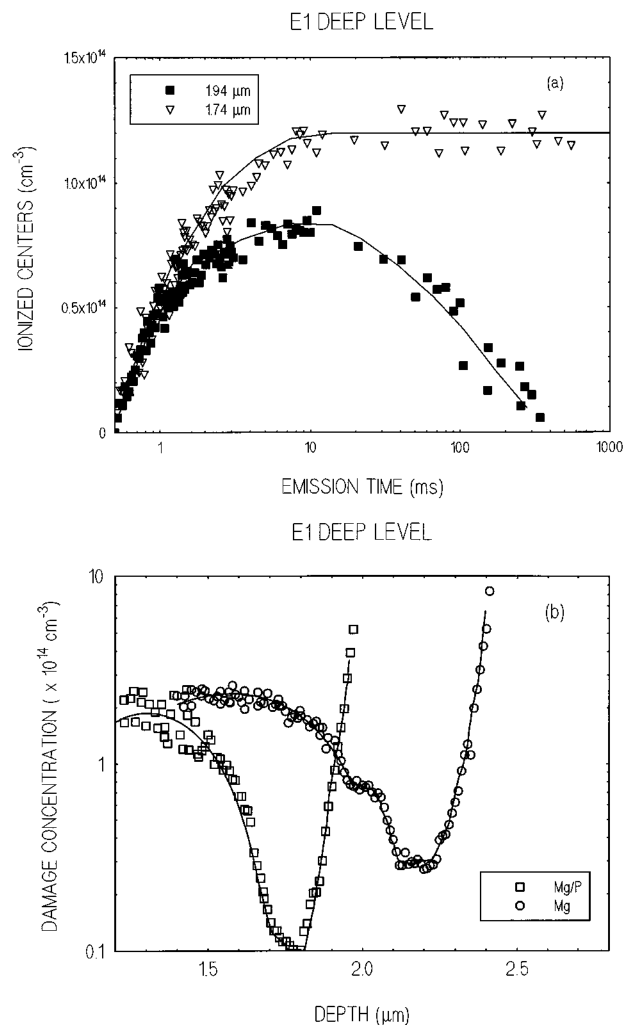

FIG. 4. (a) Emission transients of the E1 deep level for the Mg-implanted sample as a function of the emission time at different positions across the space-charge region. (b) CVTT damage concentration profile of the E1 deep level for the Mg and Mg/P implanted samples.

Several important conclusions based on the distortion of the E1 emission transients in all the samples can be extracted. First, the RTA process induces the H1 level, and any possible influence of the implantation process should be excluded. And, second, the emission process of the E1 center is completely distorted by the H1 level capture process that is taking place simultaneously. As a consequence, most of the parameters derived for E1 must be considered as merely apparent, because of the E1–H1 interaction.

2. E2 and E3 levels

The levels E2 and E3 at energies of 0.45 and 0.425 eV, respectively, could be related to phosphorus vacancies (V_P) or complexes with V_P, which are the most probable defects created in InP after annealing.[20] Several studies[10,21,22] support this assignment.

The E2 and E3 levels of the annealed and unimplanted sample show similar profiles (Figs. 5 and 6). In both cases, a slightly decreasing profile along with similar concentrations are observed. However, important differences must be pointed out for the implanted samples. For the E2-labeled

Copyright ©2001. All Rights Reserved.

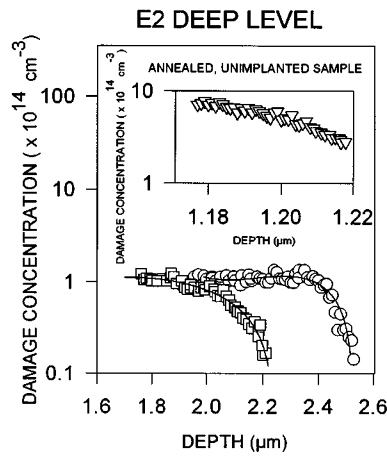

FIG. 5. CVTT damage concentration profile of the E2 deep level for the Mg (○) and Mg/P (□) implanted samples. In the insert, the E2 damage profile for the annealed and unimplanted (control) sample has been included for comparison.

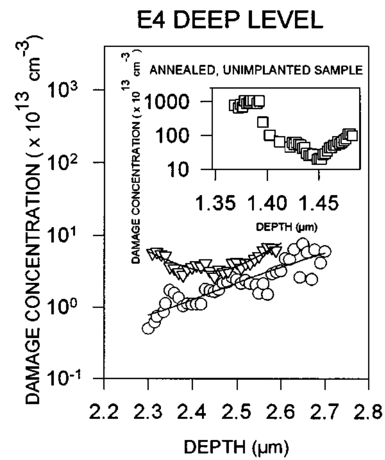

FIG. 7. CVTT damage concentration profile of the E4 deep level for the Mg (○) and Mg/P (▽) implanted samples. In the insert, the E4 damage profile for the annealed and unimplanted (control) sample has been included for comparison.

center, large trap density gradients are found in the implanted samples (Fig. 5). The sharp descending slope appears before in the space-charge region for the Mg/P coimplanted than for the Mg implanted sample (at around 2.1 and 2.4 μm, respectively). Moreover, the E2 concentrations in these samples are similar and lower than that of the control sample. A complex defect involving some residual impurity present in the InP substrate should be not excluded. The abrupt drop of the concentration may be indicative of an outward-diffusion process of this impurity. As the profile depletion appears before in the space-charge region for the coimplanted (most damaged) samples, we suggest that the residual impurity may be some transition metal whose fast diffusing interstitials are more mobile when going through heavily damaged regions.[11] Conversely to E2, the E3 level disappears after the implantation process. A change in its nature may be proposed to explain this behavior.

3. E4 level

Several authors[21,23,24] have found a level around 0.24 eV below the conduction band, which could resemble the E4 center. However, no origin was suggested.

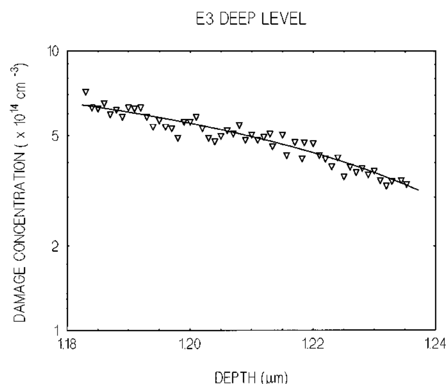

FIG. 6. CVTT damage concentration profile of the E3 deep level for the annealed and unimplanted (control) sample.

In Fig. 7, we show E4 level profiles for three kinds of samples: unimplanted, Mg implanted, and Mg/P coimplanted. Two experimental results should be pointed out. First, the nonuniform distribution of the damage concentration of this level in the control sample, in contrast to the relatively uniform character for both implanted samples, and, second, the notably higher value of the damage concentration in the former sample with respect to the others (two orders of magnitude). This conclusion agrees with the great discrepancy found in the DLTS peak amplitudes. Although the physical origin of this center is directly related to the thermal treatment, it is difficult to assign a more precise microscopic origin. For the implanted samples, no density gradient is observed in the scanned area of the space-charge region. Therefore, migration of residual impurities seems not to be directly involved. Moreover, no important differences are observed between implanted and coimplanted samples. Also, the E4 level is not affected by phosphorus coimplantation. It has been shown[11] that thermal treatments induce outward migrations of residual impurities initially located at indium sites. So, a layer of indium vacancies exists deep into the bulk after annealing. Simultaneously, Mg-implanted dopants undergo an inward diffusion based on an interstitial-substitutional mechanism.[11] Mg interstitials penetrate into the bulk and become substitutional, occuping indium sites. Thus, the indium vacancy concentration diminishes. Because of the notable reduction of the damage concentration of the E4 level that is experimentally observed in the implanted samples, we suggest that the E4 origin might be related to these indium vacancies.

4. E5 level

The E5 level, which appears as a shoulder of the dominant E1 center in the Mg-implanted sample and becomes very clear in the Mg/P coimplanted sample, could be similar to the level reported by Levinson *et al.*,[25] although they estimated an activation energy around 0.7–0.9 eV. A better

Copyright ©2001. All Rights Reserved.

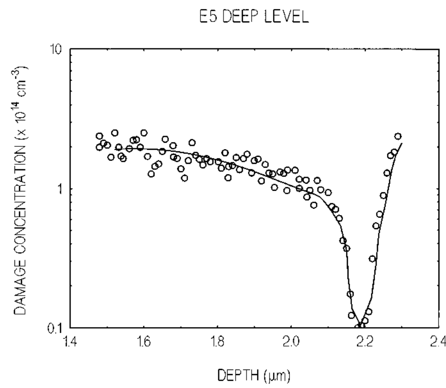

FIG. 8. CVTT damage concentration profile of the E5 deep level for the Mg/P implanted sample.

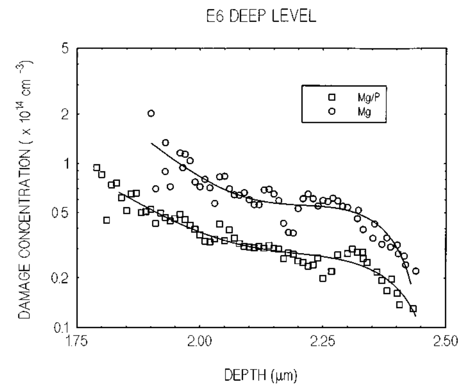

FIG. 9. CVTT damage concentration profile of the E6 deep level for the Mg and Mg/P implanted samples.

coincidence in the energy value is obtained when comparing it with the level located at 0.45 eV below the conduction band described by Kringhoj.[26]

As this trap is observed distinctly from E1 only in the coimplanted sample, CVTT curves were not recorded in the Mg-implanted sample.

Similarly to the E1 center, the E5 emission transients were collapsed at certain points of the space-charge region. The profile plotted in Fig. 8 indicates a uniform damage concentration until 2 μm. Afterward, an abrupt decrease, located at the space-charge region and followed by a rapid recovery, is observed. Again, no clear E5 characteristic can be extracted from its emission transients because of the distortion induced by the capture process of H1.

If a detailed comparison of the dopant profiles of E1 and E5 for the Mg/P coimplanted samples [Figs. 4(b) and 8] is carried out, a different spacial location of the profile depletion can be noticed. This fact is due to the different temperature at which the CVTT measurements were recorded (room temperature and 260 K, respectively). When the temperature rises, the extension of the space-charge region decreases. Thus, the edge zone of the space-charge region, where free carrier electrons exist, shifts in position. Therefore, the delicate balance between the E1 electron emission and the H1 electron capture may be unbalanced by the temperature and, therefore, the location of the depletion profile varies.

5. E6 level

Two levels reported in the literature could resemble the E6 level: the 0.24 eV level of Suski *et al.*,[27] the 0.22 eV level of Levinson *et al.*[25]

In Fig. 9, damage profiles for this level display a nonuniform distribution and the gradual decrease penetrating deep into the space-charge region must be noticed. Moreover, the concentration is higher for the Mg-implanted samples than for the Mg/P coimplanted ones. Radiation damage may be proposed as a probable origin for this trap. It would be expected that when damage increases, trap concentration does also. Therefore, this damage density should be increased for the coimplanted samples. Yet, this argument does not agree with the profiles shown in Fig. 9. Another option can be proposed, taking into account that the level only appears for the implanted samples: the Mg dopant may participate in the formation of deep levels. Moreover, complex defects of Mg with other species, where intrinsic defects are excellent candidates, cannot be discarded. The densely damaged regions of the Mg/P coimplanted sample prevent a deeper penetration of the Mg interstitials.[5] Therefore, a lower concentration of Mg is found deep into the bulk. Thus, we may conjecture that a certain interaction appears between the implanted ions and intrinsic defects, such as the annealing-induced E3 level, which vanished in the implanted samples, giving rise to a complex defect.

6. E7 level

The 0.28 eV level of Kringhoj[26] found in n^+-p InP junctions made by Ge implantation and RTA, as well as the frequency dispersion in the gain of a fully ion-implanted InP JFET with an activation energy of 0.28 eV reported by Kruppa *et al.*,[28] may be correlated with the E7 center.

The nonuniformity of profiles in Fig. 10, increasing their concentration toward the bulk, should be pointed out. It is worth remarking that the analogous evolution of the profiles occurs for both samples. Similar damage concentration values are found, although this damage tends to be slightly higher for the Mg-implanted one. From these results, some potential physical origins may be excluded. First, as the coimplantation does not produce a clearly higher damage

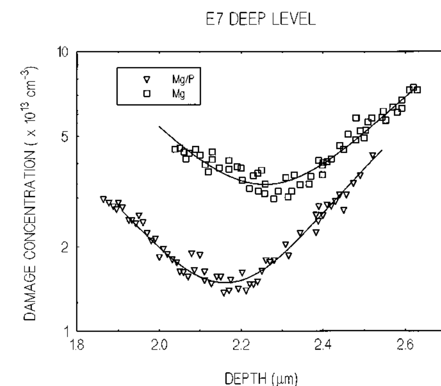

FIG. 10. CVTT damage concentration profile of the E7 deep level for the Mg and Mg/P implanted samples.

Copyright ©2001. All Rights Reserved.

concentration, radiation-induced defects seem not to be implicated. And, second, the increase of the profile toward the bulk seems to suggest that Mg-implanted atoms do not participate in this level. Owing to the abrupt profile evolution across the space-charge region, clusters or even dislocation loops associated with implantation and diffused by subsequent annealing might be suggested.

B. Emission coefficients

Deep levels in semiconductor materials are often characterized by measuring the thermal emission and capture rates of carriers in the depletion region. It has been extensively observed that the emission rate depends on the electric field in the space-charge region when this field reaches high enough values. Several physical origins have been proposed as cause of the electric field dependence of the emission rate, namely, Poole–Frenkel barrier lowering, tunneling effects, and electron-phonon tunneling.[29] For the highest electric fields ($>10^6$ V/cm), pure tunneling is the dominant effect, whereas for lower values, the other mechanisms are prevalent.[29] The fields existing across the space-charge region in the present work never exceed the value of 2×10^4 V/cm near the junction. Therefore, the second mechanism is unlikely to occur. In addition to the electric field dependence of the emission coefficients, other physical phenomena, such high deep level concentrations, nonuniform distributions, refilling effects, and so on,[16,17] can produce nonexponential emission transients. As an important result, the emission transients showed a single exponential character for all the centers and samples studied.

In Figs. 11(a) and 11(b), we show the emission rates distributions for the different deep levels at temperatures where they emit electrons. Two different groups can be distinguished according to their emission rate profiles. For E2, E3, and E6 levels, no important changes of the emission coefficient are detected. For E4 and E7, this parameter increases going to the bulk; this trend is more evident for E7.

The electric field dependence exhibited by the first group of centers can be accounted for by suggesting that the fields used in this study were not high enough to produce significant differences. However, it is appropriate to mention here that additional mechanisms can alter and even suppress electric field-induced barrier lowering. Buchwald and Johnson[30] proposed that this behavior is related to a thermally activated cross section for electron capture. In this sense, Wada *et al.*[22] have shown that different deep levels in InP exhibit this peculiar behavior (their A, D, and E-labeled levels). In particular, we have correlated their E level with our E3 one, which corresponds to the group of the levels where nonapparent electric field dependence exists. On the other hand, the rather similar values of the emission rate for samples submitted to different technology processes prove the identical physical nature of the corresponding centers.

As far as the E4 and E7 levels are concerned, their evolution is contrary to a Poole–Frenkel mechanism. A thermally activated tunneling mechanism might be invoked to explain the decrease of the emission rate when the electric field increases. This kind of conduction mechanism was suggested in a previous work[31] to properly fit reverse $I-V$ characteristics at different temperatures for similarly implanted junctions. The best fitting obtained by simulation for the experimental results was achieved with an energy value of around 0.3 eV which could agree with our E7 level ($E_{E7}=0.27$ eV).

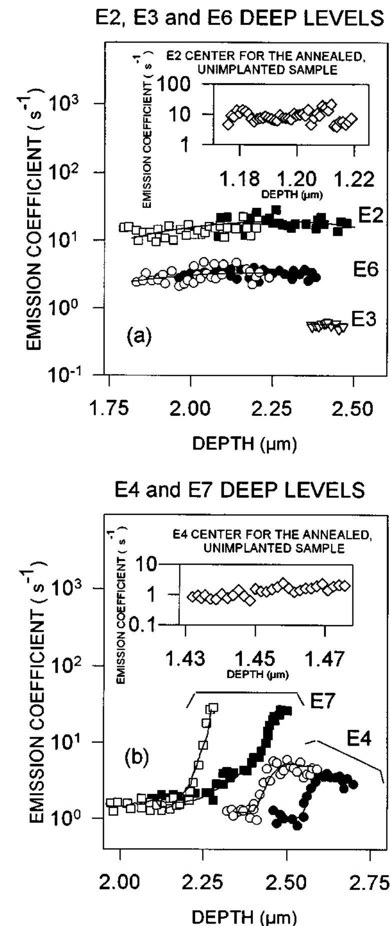

FIG. 11. CVTT emission rate distribution for: (a) E2, E3, and E6 deep levels. Abscisa coordinates for the E3 center data (▽) have been multiplied by 2 in order to be included in the same range as E2 and E6; (b) E4 and E7 deep levels. For the E2 and E4 centers, the emission rate distribution for the control sample has been included in the insert for comparison. In both (a) and (b), full symbols correspond to the Mg-implanted samples and hollow symbols to the Mg/P implanted ones.

V. CONCLUSIONS

Seven electron levels (E1 at 0.6 eV, E2 at 0.45 eV, E3 at 0.425 eV, E4 at 0.2 eV, E5 at 0.46 eV, E6 at 0.25 eV, and E7 at 0.27 eV below the conduction band) and one hole level (H1 at 1.33 eV above the valence band) have been detected in the upper half of the band gap in p^+-n InP junctions fabricated by RTA of Mg or Mg/P implanted substrates. These levels were characterized using DLTS and CVTT.

From the DLTS spectra, the majority traps were classified in two groups, according to their physical origin: E1, E2, E3, and E4 were associated to RTA-induced centers, and E5, E6, and E7 were ascribed to ion implantation-induced levels.

From the CVTT analysis, several characteristics of each trap were derived in order to get further insight into its physical nature. The E1 level could be related to Fe. Its electron

Copyright ©2001. All Rights Reserved.

emission process was totally distorted by the simultaneous electron capture due to the H1 level, which appears at the same temperature range as E1 and is energetically located quite near the conduction band. The H1 level was ascribed to a RTA-induced origin, as the distortion of the E1 emission transient also exists for the annealed and unimplanted sample. A similar distortion was found in the emission of the E5 level. As the E2 and E3 levels were found to appear just after a RTA treatment, these traps are probably related to V_P or complexes with V_P. The remarkable difference of the E4 damage concentration between the unimplanted and implanted samples suggests the tentative relation of this center to indium vacancies. The E6 and E7 levels were tentatively associated with Mg implanted atoms and implantation-originated clusters or dislocation loops, respectively.

As far as the emission properties of the centers, two conclusions were drawn. First, the emission transients showed a single exponential character for all the centers and samples studied. And, second, two groups of centers were considered according to the evolution of its emission rate across the depletion region. For the E2, E3, and E6 levels, no significant change was detected. Regarding the E4 and E7 levels, a thermally activated tunneling mechanism was suggested to justify the emission rate distribution increase with increasing depth in the bulk.

[1] W. Kruppa and J. P. Boos, IEEE Electron Device Lett. **8**, 223 (1987).
[2] J. P. Boos, W. Kruppa, and B. Molnar, IEEE Electron Device Lett. **10**, 79 (1989).
[3] B. Molnar, T. A. Kennedy, E. R. Glaser, and H. B. Dietrich, J. Appl. Phys. **74**, 3091 (1993).
[4] M. Gauneau, R. Chaplain, H. L'Haridon, M. Salvi, and N. Duhamel, Nucl. Instrum. Methods B **19**, 418 (1987).
[5] M. V. Rao and R. K. Nadella, J. Appl. Phys. **67**, 1761 (1990).
[6] K. W. Wang, Appl. Phys. Lett. **51**, 2127 (1987).
[7] H. Shen, G. Yang, Z. Zhou, C. Lin, and S. Zou, IEEE Electron Device **39**, 209 (1992).
[8] J. M. Martín, S. García, F. Calle, I. Mártil, and G. González-Díaz, J. Electron. Mater. **24**, 59 (1995).
[9] K. L. Jiao, A. J. Soltyka, and W. A. Anderson, Appl. Phys. Lett. **57**, 1913 (1990).
[10] E. K. Kim, H. Y. Cho, J. H. Yoon, S. Min, Y. L. Jung, and W. H. Lee, J. Appl. Phys. **68**, 1665 (1990).
[11] R. Chaplain, M. Gauneau, H. L. Haridon, and A. Rupert, J. Appl. Phys. **58**, 1803 (1985).
[12] M. Gauneau, H. L'Haridon, A. Rupert, and M. Salvi, J. Appl. Phys. **53**, 6823 (1982).
[13] S. Dueñas, E. Castán, L. Enríquez, J. Barbolla, J. Montserrat, and E. Lora-Tamayo Semicond. Sci. Technol. **9**, 1637 (1994).
[14] S. Dueñas, E. Castán, L. Quintanilla, L. Enríquez, J. Barbolla, E. Lora-Tamayo, and J. Montserrat, Mater. Sci. Technol. **11**, 1074 (1995).
[15] S. Dueñas, R. Pinacho, L. Quintanilla, E. Castán, J. Barbolla, J. Montserrat, and E. Lora-Tamayo (unpublished).
[16] S. D. Brotherton, J. P. Gowers, N. D. Young, J. B. Clegg, and J. R. Ayres, J. Appl. Phys. **60**, 3567 (1986).
[17] L. Enríquez, S. Dueñas, J. Barbolla, I. Izpura, and E. Muñoz, J. Appl. Phys. **72**, 525 (1992).
[18] J. M. Martín, Ph.D. thesis, University Complutense, Madrid, 1994.
[19] J. Cheng, S. R. Forrest, B. Tell, D. Wilt, B. Schwartz, and P. Wright, J. Appl. Phys. **58**, 1787 (1985).
[20] J. D. Oberstar and B. G. Streetman, Thin Solid Films **103**, 17 (1983).
[21] N. Yamamoto, K. Uwai, and K. Takahei, J. Appl. Phys. **65**, 3072 (1989).
[22] O. Wada, A. Majerfeld, and A. N. M. Choudhury, J. Appl. Phys. **51**, 423 (1980).
[23] M. A. A. Pudensi, K. Mohammed, and J. L. Merz, J. Appl. Phys. **57**, 2788 (1985).
[24] H. Asahi, Y. Kawamura, M. Ikeda, and H. Okamoto, J. Appl. Phys. **52**, 2852 (1981).
[25] M. Levinson, J. L. Benton, H. Temkin, and L. C. Kimerling, Appl. Phys. Lett. **40**, 990 (1982).
[26] P. Kringhoj, Mater. Sci. Eng. B **9**, 315 (1991).
[27] J. Suski, J. C. Bourgoin, and H. Lim, J. Appl. Phys. **54**, 2852 (1983).
[28] W. Kruppa, J. B. Boos, and T. F. Carruthers, Proceedings of the III International Conference on InP and Related Materials, Cardiff U.K., IEEE Catal. 91CH2950-4 (1991) (unpublished).
[29] G. Vincent, A. Chantre, and D. Bois, J. Appl. Phys. **50**, 5484 (1979).
[30] W. R. Buchwald and N. M. Johnson, J. Appl. Phys. **64**, 958 (1988).
[31] J. M. Martín, S. García, I. Mártil, G. González-Díaz, E. Castán, and S. Dueñas, J. Appl. Phys. **78**, 5325 (1995).

Copyright ©2001. All Rights Reserved.